Operational Forecasting of Wind-Generated Waves by Hurricane Isabel at NCEP*

HENDRIK L. TOLMAN,+ JOSE-HENRIQUE G. M. ALVES,+ AND YUNG Y. CHAO

Marine Modeling and Analysis Branch, NOAA/NCEP/Environmental Modeling Center, Camp Springs, Maryland

(Manuscript received 5 March 2004, in final form 10 September 2004)

ABSTRACT

The accuracy of the operational wave models at the National Centers for Environmental Prediction (NCEP) for sea states generated by Hurricane Isabel is assessed. The western North Atlantic (WNA) and the North Atlantic hurricane (NAH) wave models are validated using analyzed wind fields, and wave observations from the *Jason-1* altimeter and from 15 moored buoys. Both models provided excellent guidance for Isabel in the days preceding landfall of the hurricane along the east coast of the United States. However, the NAH model outperforms the WNA model in the initial stages of Isabel, when she was a category 5 hurricane. The NAH model was also more accurate in providing guidance for the swell systems arriving at the U.S. coast well before landfall of Isabel. Although major model deficiencies can be attributed to shortcomings in the driving wind fields, several areas of potential wave model improvement have been identified.

1. Introduction

Hurricane Isabel made landfall on the east coast of the United States near Cape Hatteras on 18 September 2003 (see Fig. 1). Due to the size and intensity of Isabel, extreme wave conditions were observed and predicted along the coast. Significant wave heights greater than 10 m were observed about 250 nm offshore at National Data Buoy Center (NDBC) buoys 41001 and 41002, which were located on either side of the corridor of predicted maximum wave heights. NDBC buoy 41025, located in the path of predicted maximum wave heights, was rendered inoperative well before the most extreme wave conditions were reached. The operational wave models at the National Centers for Environmental Prediction (NCEP) predicted wave heights at this buoy of up to 15 m. Extreme wave conditions extended along the coast. At a waverider buoy only 2 n mi offshore at the Field Research Facility (FRF) of the U.S. Army Corps of Engineers at Duck, North Carolina (information available online at http://www.frf.usace.army.mil), wave heights of up to 8.1 m were observed. Wave heights of more than 4 m were observed as far south as buoy 41009 and as far north as buoy 44011 (see Fig. 1).

In this paper we review the performance of the guidance forecasts produced by the operational regional wind–wave models for the western North Atlantic Ocean domain at NCEP during the life cycle of Hurricane Isabel. NCEP has provided numerical wind wave guidance for several decades (Tolman et al. 2002). Presently two regional models with a spatial resolution of 0.25° in latitude and longitude provide guidance for the North Atlantic region. These are the western North Atlantic model (WNA) and the North Atlantic hurricane wave model (NAH) (Chao et al. 2003a,b).

This study focuses on these two models, which use identical spatial grids and spectral discretizations, but which differ in the wind forcing. This will be described in more detail in section 2. Also discussed in this section are the validation data used. Because the accuracy of wave forecasts is heavily dependent on the quality of the driving wind fields, the accuracy of wind fields is assessed in section 3, before model wave height predictions are compared with buoy and altimeter data in

* Marine Modeling and Analysis Branch Contribution Number 245.

+Additional affiliation: Science Applications International Corporation/GSO, Beltsville, Maryland.

Corresponding author address: Hendrick L. Tolman, NOAA/NCEP/Environmental Modeling Center, Rm. 209, 5200 Auth Rd., Camp Springs, MD 20746.
E-mail: Hendrik.Tolman@NOAA.gov

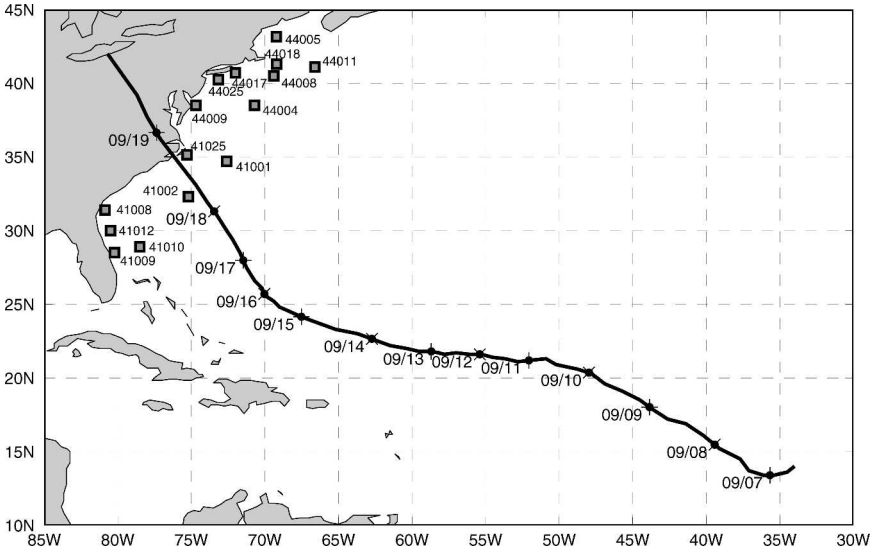

FIG. 1. Buoy locations used in this study and the best-guess track of Hurricane Isabel. Dates along track correspond to 0000 UTC.

section 4. A discussion and conclusions are presented in sections 5 and 6, respectively. Additional information on the performance of NCEP's wave models for Isabel can be found in Tolman et al. (2004, hereafter TAC).

2. Models and data

Operational wave forecast guidance is provided at NCEP by the National Oceanic and Atmospheric Administration's (NOAA) WAVEWATCH III (NWW3) model suite, which consists of a global model and several nested regional models. This investigation focuses attention on the WNA and NAH models, both of which are based on version 2.22 of the WAVEWATCH III model (Tolman 2002a,c; Tolman et al. 2002). These implementations of WAVEWATCH III use the default model setting as defined in Tolman (2002c) with few exceptions. Details of the model setup, including deviations from the default settings of WAVEWATCH III, are shown in Table 1. Additional information for these two models can be found in Chao et al. (2003a,b).

Input for the wave models consists of wind fields at 10-m height above the sea surface and ice concentration fields. The latter are obtained from NCEP's automated passive microwave sea ice concentration analysis (Grumbine 1996) and are updated daily. Wind fields are generally provided by NCEP's Global Forecast System (GFS; see, e.g., Caplan et al. 1997; Moorthi et al. 2001) and are available at 3-h intervals and presently have a spectral resolution of T254. This corresponds to a spatial resolution of approximately 50 km, which is significantly poorer than the 25-km resolution of the wave models. For the NAH wave model, high-resolution wind fields, generated hourly at NCEP by the Geophysical Fluid Dynamics Laboratory (GFDL) model for individual hurricanes, are blended with 3-hourly GFS wind fields. For this purpose, hourly GFS wind fields are generated by interpolation. The blending scheme is described in detail in Chao et al. (2005, hereafter CAT05). The GFDL wind fields have a spatial resolution of 1/6° near the hurricane, but are effectively used at the 25-km resolution of the wave models. The GFDL model winds are more appropriate for forcing a hurricane wave model mostly due to the better spatial resolution (see CAT05).

TABLE 1. Implementation details of the operational regional WAVEWATCH III models for the North Atlantic Ocean at NCEP. The nonstandard options are name lists as used in the input file of the ww3_grid component of WAVEWATCH III; d_{min} is the smallest water depth allowed in the model.

Model	Grid	d_{min} (m)	Nonstandard WAVEWATCH III options
WNA	0°–50°N 98°–30°W 0.25° × 0.25°	7.5	&sbt1 gamma = −0.019/ &misc flagtr = 4, cice0 = 0.25, cicen = 0.75/
NAH	0°–50°W 98°–30°W 0.25° × 0.25°	7.5	&sbt1 gamma = −0.019/ &misc flagtr = 4, cice0 = 0.25, cicen = 0.75/ &pro3 wdthcg = 2.00, wdthth = 2.00/

The quality of these different wind fields is assessed using independent analyses of surface winds for Isabel from the Hurricane Research Division (HRD) of the Atlantic Oceanographic and Meteorological Laboratory (AOML) of NOAA (Powell et al. 1996, 1998). All data used here have been obtained from the HRD Web site (information available online at http://www.aoml.noaa.gov/hrd). These wind fields formally represent 1-min-average wind speeds. To become more representative for (sustained) model wind fields, they have been converted to 10-min-average wind speeds using the approach described in Powell et al. (1996).

The AOML analyses are produced interactively, requiring human intervention. Generally, they are available for hurricanes at 6-h intervals, but not always at fixed times. Note that no AOML analyses are available for the first 5 days of Isabel's 13-day life cycle over ocean waters. Best-track information and independent maximum wind speed estimates were obtained from NCEP's Tropical Prediction Center (TPC; Beven and Cobb 2003). The latter wind speeds were also converted from 1- to 10-min-average values, following Powell et al. (1996).

Traditionally, wave models are validated using data from buoys. In the present study, we use the data from NDBC for buoy locations shown in Fig. 1. Although these data are received at NCEP in near–real time as part of the operational data stream, quality controlled data can also be obtained from the NDBC Web site (information available online at http://www.ndbc.noaa.gov). We have used the latter data for the present study.

Buoy data are generally available near most coastal areas of the United States, but they do not provide adequate coverage over the deep ocean areas. Global wave height data for deep water locations may, however, be obtained from altimeters on board satellites. At the time of Isabel, altimeter data were available from the *Jason-1* satellite. The *Jason-1* data used here were retrieved from the historical archive at the Naval Research Laboratory (NRL), through their Web (http://www7320.nrlssc.navy.mil) and ftp (ftp://ftp7320.nrlssc.navy.mil) servers. These altimeter data do not show relevant biases for any wave height (e.g., Ray and Beckley 2003), as was confirmed independently by altimeter–buoy collocations at NCEP (figures not presented here). In fact, these altimeter data can be considered to be of similar quality as in situ buoy observations.

All buoy and altimeter data are used here at their original resolution, that is, without additional averaging, unless specified differently.

3. Isabel's surface wind fields

The tropical system Isabel was in existence over Atlantic waters from 6 through 19 September 2003 (see Fig. 1 and Beven and Cobb 2003). Isabel became a category 1 hurricane on 7 September, was a category 5 hurricane from 11 (when the first AOML data became available) through 14 September, and became a category 2 hurricane from 16 through 18 September. We will discuss the quality of the wind fields used by the WNA and NAH models using best-track and track envelope information (Fig. 2), the corresponding maximum wind speed envelopes (Fig. 3), and selected example wind fields (Fig. 4). The envelope information will consider 0–72-h forecasts, corresponding to the forecast horizon of the NAH model.

Track forecasts of Isabel from both the GFDL and GFS models, as presented in Fig. 2, in general are excellent, mostly due to the predictable nature of Isabel (see Beven and Cobb 2003). From 7 through 14 September, the track envelope of the GFDL (NAH, Fig. 2a) model is narrower, indicating a better forecast. Near landfall, the GFDL (NAH) model displays a bias to the left of the track that is not observed in the GFS (WNA, Fig. 2b) model.

The most relevant intensity parameter of a hurricane for wind–wave generation is the maximum wind speed. Figure 3 shows the maximum wind speeds of the AOML and TPC analyses (symbols), the analysis or hindcast wind fields (solid lines), and the range of wind speeds for each valid time for forecasts up to 72 h (shaded area) for the GFS (WNA) and GFDL (NAH) models.

While Isabel is a category 5 hurricane (11–15 September), both models systematically underestimate the maximum wind speeds compared to the AOML and TPC analyses. The GFDL (NAH) model (Fig. 3a) nevertheless represents Isabel's wind speed much more realistically than does the GFS (WNA) model (Fig. 3b). The analysis wind fields appear most realistic, whereas the forecasts systematically underestimate the maximum wind speeds.

Near landfall (16–19 September), both the GFS (WNA) and GFDL (NAH) models closely reproduce the maximum wind speeds from the AOML and TPC analyses. Forecast maximum wind speeds for the GFS (WNA) model are still systematically lower than analyzed maximum wind speeds, but the differences are much smaller than in the earlier stages of Isabel's life cycle.

For accurate wave forecasting both the maximum wind speeds and spatial scales of the hurricane are important, because the maximum wave height is a func-

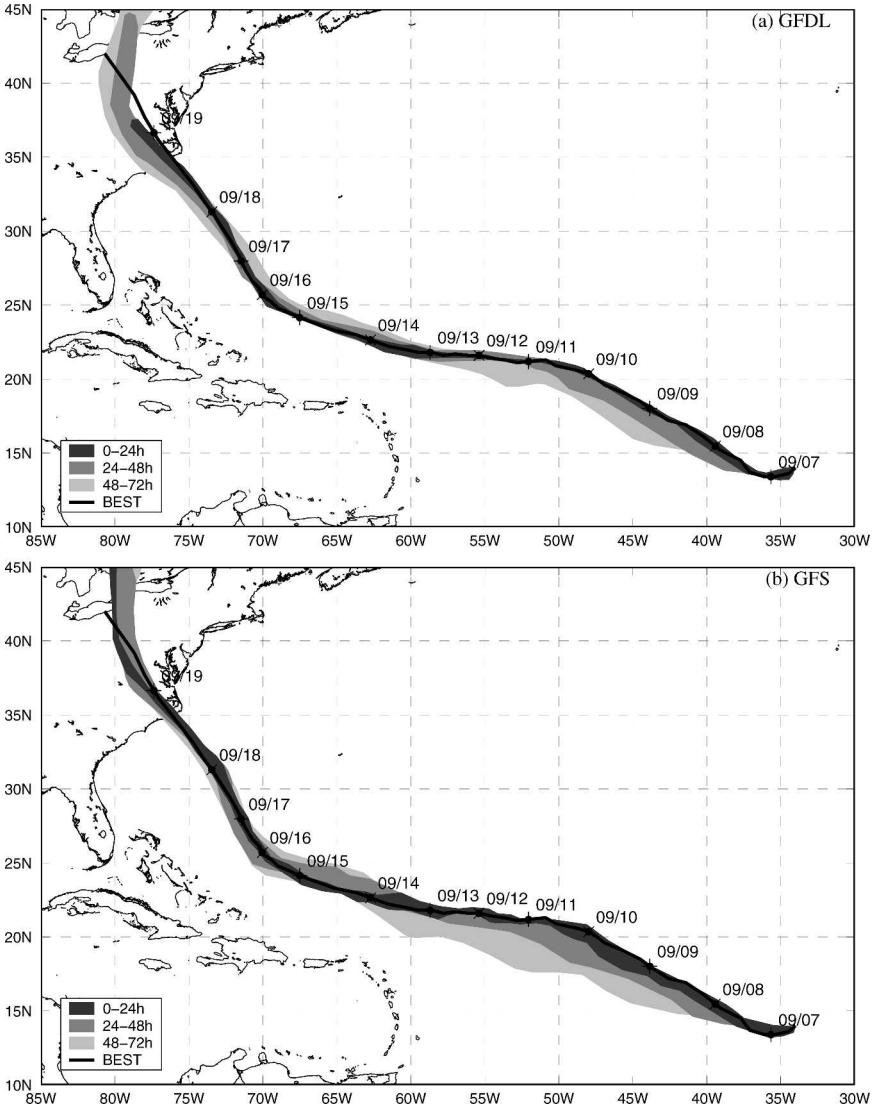

FIG. 2. Track forecasts for Isabel from (a) the GFDL (NAH) model and (b) the GFS (WNA) model. Shading identifies tracks for various forecast ranges. Best track from TPC.

tion of wind speed, fetch, and forward motion of the hurricane (e.g., Young 2003). The representation of the structure of Isabel by the GFDL and GFS models is illustrated with analyzed wind fields in Fig. 4 using three examples.

On 13 September (upper panels in Fig. 4), the GFDL model captures the structure of Isabel, but underestimates the intensity (see Fig. 3a). The GFS model fails to capture Isabel realistically. On 15 September (middle panels in Fig. 4), the GFDL model captures the intensity accurately, but underestimates the spatial scale. The GFS model captures the spatial structure accurately, but still underestimates the intensity. On 17 September, both models provide a realistic representation of Isabel. Inspection of all available analyses and of Fig. 3 suggests that in the 3 days before landfall, the GFDL model appears to capture the intensity accurately, but underestimates the spatial scales. In contrast, the GFS model captures the spatial scales better, but underestimates wind speeds in general. Both deficiencies are small, and in general Isabel is represented realistically in both models.

For wave model forecasts, the final critical aspect of the hurricane wind field forecast is the timing of Isabel's motion along the track. This will be addressed in the following section through the analysis of wave height forecast envelopes at selected buoy locations.

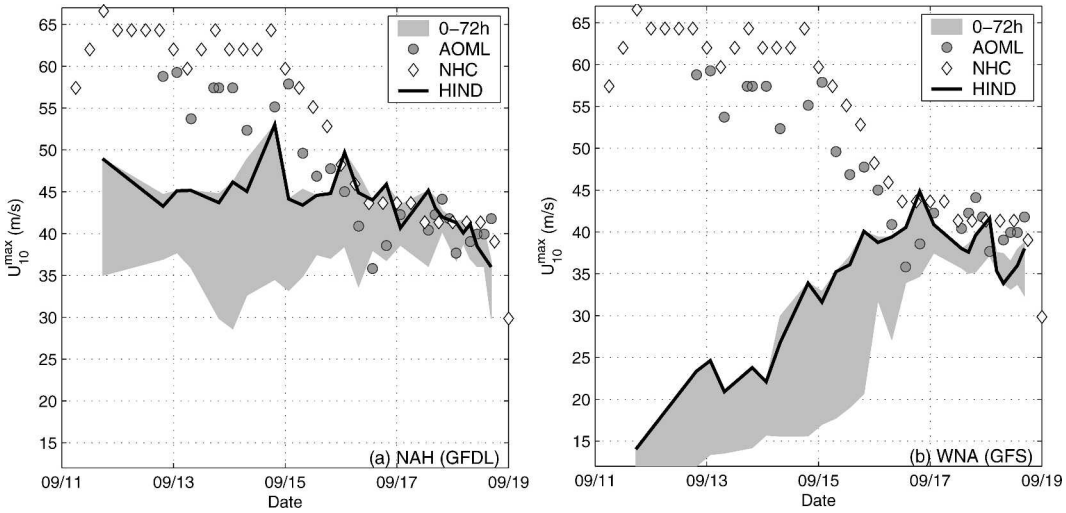

FIG. 3. Maximum wind speed ranges during the forecast from (a) the NAH (GFDL) model and (b) the WNA (GFS) model compared to maximum wind speeds from the AOML analyses and the TPC final estimates.

4. Wave prediction

The validation of the wave models will concentrate on the significant wave height H_s. Peak periods, as often used in validation, will not be considered here; due to their discontinuous nature, validation using peak periods is often misleading. Spectral data have been considered in TAC to trace the sources of swell fields and corresponding wave model errors, but for conciseness will not be presented here. The assessment of predicted wave heights will consider deep ocean hindcasts using *Jason-1* data, fore- and hindcasts using buoy data, as well as some full spatial wave height fields.

Figure 5 shows results of the NAH and WNA model hindcasts collocated with observed wave heights on selected *Jason-1* altimeter tracks. The upper two sets of panels in Fig. 5 consider tracks close to the eye of Isabel. The bottom set of panels in the figure deals with swells traveling ahead of Isabel. On 13 September, the GFS model does not yet capture Isabel realistically (see previous section). Consequently, the WNA model severely underestimates the wave heights generated by Isabel (Fig. 5a, left and right panels). However, the NAH (GFDL) model represents the wave field generated by Isabel accurately, although the representation of the most extreme wave heights cannot be validated accurately due to dropouts in the *Jason-1* data. The apparent underestimation of the wind–wave field generated by Isabel in the WNA model implies that the early swell arrivals at the buoys are expected to be severely underestimated in the WNA model.

Figures 5b represent Isabel near landfall on 17 September. At this time, GFS and GFDL wind fields are similar and of good quality, as discussed in the previous section. Consequently, the WNA and NAH wave models produce similar wave fields, closely reproducing the *Jason-1* observations. The *Jason-1* data show a sharp drop in the wave heights near the eye of Isabel. This drop is reproduced with high accuracy by both wave models, in spite of the fact that the resolution of the wave model (25 km) is significantly poorer than the along-track resolution of the altimeter (7 km).

Figures 5c present data from *Jason-1* for a combination of wind seas and swell ahead of Isabel on 15 September. At this time, the WNA model represents the structure of Isabel realistically, but still underestimates the wind speeds and corresponding wave heights systematically (as in the preceding days). Not surprisingly, the WNA model underestimates wave heights observed by *Jason-1* ahead of Isabel (dashed lines and symbols in right panel). The NAH model, however, realistically represents the wave heights (solid lines and symbols in right panel). Note that the altimeter data in Fig. 5c show distinctive spatial variability on small scales. This suggests that Isabel generated many individual swell fields. This complicates the prediction and validation of swells generated by hurricane wave models. This observed variability is not reproduced by the models.

Wave height predictions from both models for selected buoy locations are presented in Figs. 6 and 7, for the NAH and WNA models, respectively. The first four buoys (41001, 41002, 41025, and 44009) are selected for their proximity to Isabel's track. Buoys 41010 and 44011 are selected as being representative for southern and northern buoys, respectively. Buoys 41008 and

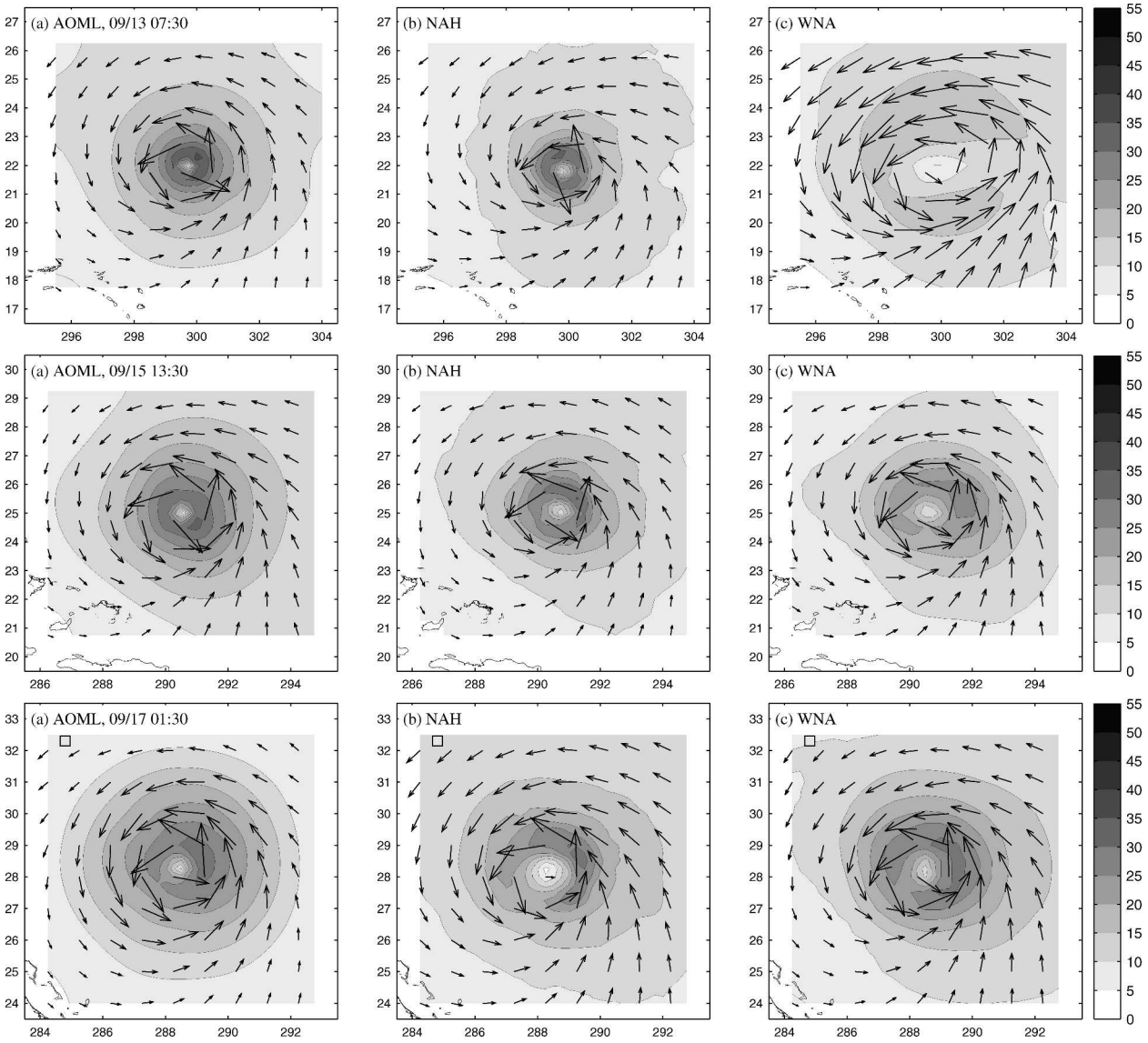

FIG. 4. Wind speeds at 10-m height in m s^{-1} for Isabel from (a) the AOML analysis, (b) the NAH model hindcast (GFDL winds), and (c) the WNA model hindcast (GFS winds). From top to bottom, the wind fields are valid for 0730 UTC 13 Sep, 1330 UTC 15 Sep, and 1030 UTC 17 Sep, respectively.

44018 are selected for their anomalous behavior. Figures 6 and 7 show the model hindcasts (solid lines) and the envelope of wave heights for the hindcast up to the 72-h forecast (shaded area). Also shown in the figures are the buoy observations. For clarity in the figures, buoy observations are displayed every 3 h and represent the averages of observations in the corresponding interval. Buoy observations are known to include a significant sampling uncertainty, due to the brevity of the time series used and the stochastic nature of wind waves (e.g., Donelan and Pierson 1983). The corresponding 95% confidence limits of the buoy data, calculated according to Young (1986), are also presented in the figures.

Spectral data as presented in TAC indicate that the first swells generated by Isabel arrive at most buoys around 12 September. Most buoys, furthermore, show a clear windsea event around 18 September, associated with Isabel. For buoys close to the track (Figs. 6a–d and 7a–d), this results in a clearly separated peak in the wave heights associated with the passage of Isabel, with a relatively short duration. For buoys farther away from the track, the largest wave heights from Isabel occur over a longer period. Two regimes with different model

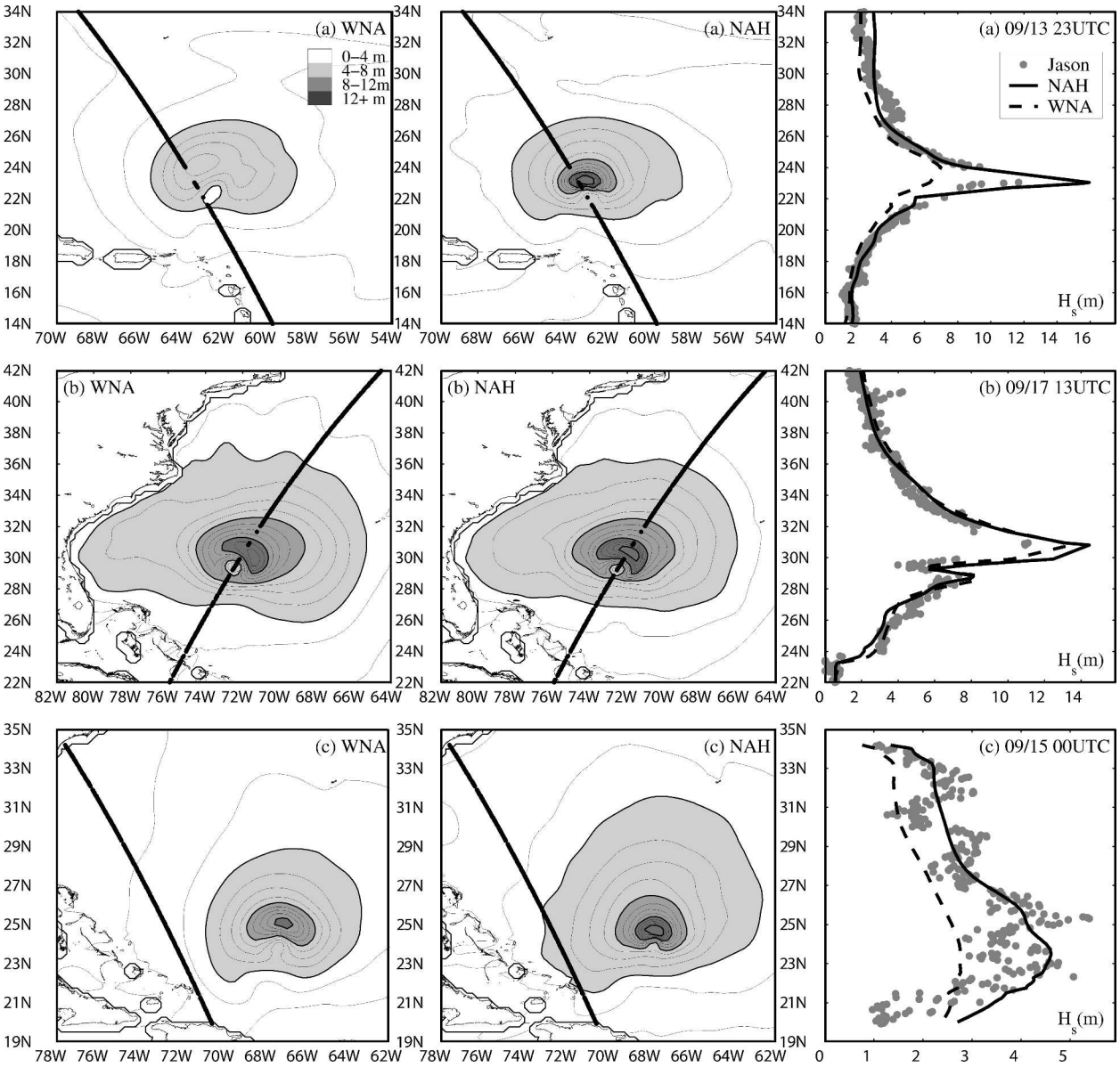

FIG. 5. Wave heights H_s in m from (left) the WNA model, (center) the NAH model, and (right) the corresponding model data collocated with *Jason-1* altimeter data for selected tracks. Model fields interpolated to the track time hour. Model and altimeter data collocated by interpolation in space and time from hourly wave height fields. The solid lines in the left and center panels represent *Jason-1* data points: (a) 2300 UTC 13 Sep, (b) 1300 UTC 17 Sep, and (c) 0000 UTC 15 Sep.

behavior can be distinguished. The first is the arrival of early swells, typically from 12 through 17 September. The second is the period with wind seas and swell associated with Isabel close to landfall, typically from 17 through 19 September. Henceforth, these two periods will simply be denoted as the first and second periods.

In the first period, the NAH model (Fig. 6) produces systematically higher swells at the buoy locations than the WNA model (Fig. 7). The NAH model generally mimics the observations more closely than the WNA model, as expected from deficiencies in the wind fields as described above. In the second period, both models represent observations accurately. Conventional validation statistics for the model hindcasts are presented in Table 2. The scatter index (SI) is defined here as the rms error normalized with the mean observation. Differences in the statistics are dominated by model behavior in the first period, and confirm that the NAH model was generally significantly more accurate.

The NAH model, nevertheless, has some clear defi-

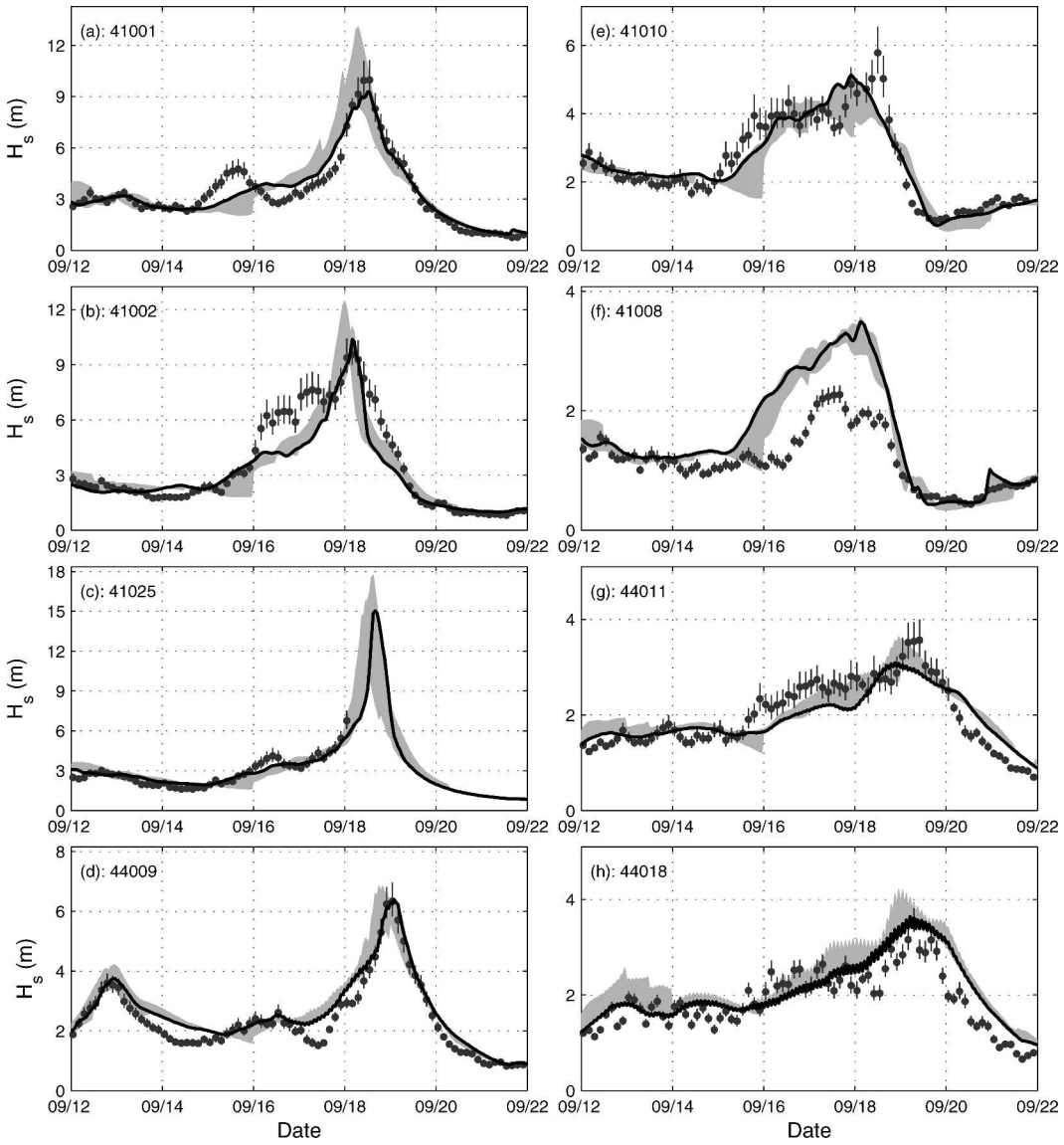

FIG. 6. Wave heights H_s at selected NDBC buoys from NAH model and buoy observations: solid line, model hindcast; shaded area, envelope of wave heights from hindcast to 72-h forecast; filled circle (●), mean observed wave height; and vertical bar (|), corresponding 95% confidence interval; at buoys (a) 41001, (b) 41002, (c) 41025, (d) 44009, (e) 41010, (f) 41008, (g) 44011, and (h) 41018.

ciencies, for instance missing swell peaks on the 15 and 16 September at buoys 41001, 41002, and 41025. Spectral analyses presented in TAC indicate that this is probably due to the underestimation of Isabel's wind speeds when she was a category 5 hurricane. Table 2, furthermore, indicates anomalous behavior at buoy 41008 (see also Figs. 6f and 7f), and to a lesser extent at buoy 41012. At these buoys, the WNA model outperforms the NAH model. This appears to be related to a systematic lack of wave energy dissipation on the southern Atlantic shelf, as confirmed by altimeter data in TAC. The more realistic (higher) offshore swells in the NAH model then result in an increased overestimation of the wave heights on the shelf. Furthermore, both models show some deficiencies at buoy 41018. The observations at this buoy (Figs. 6h and 7h) show a clear diurnal modulation, suggesting (tidal) wave–current interactions. Such interactions are not included and, therefore, not reproduced in the models. Furthermore, both models show (minor) modulations with a period of twice the model time step, indicating potential numerical "instability." Both issues will be discussed in more detail in section 5.

The forecast envelopes (shaded areas in Figs. 6 and

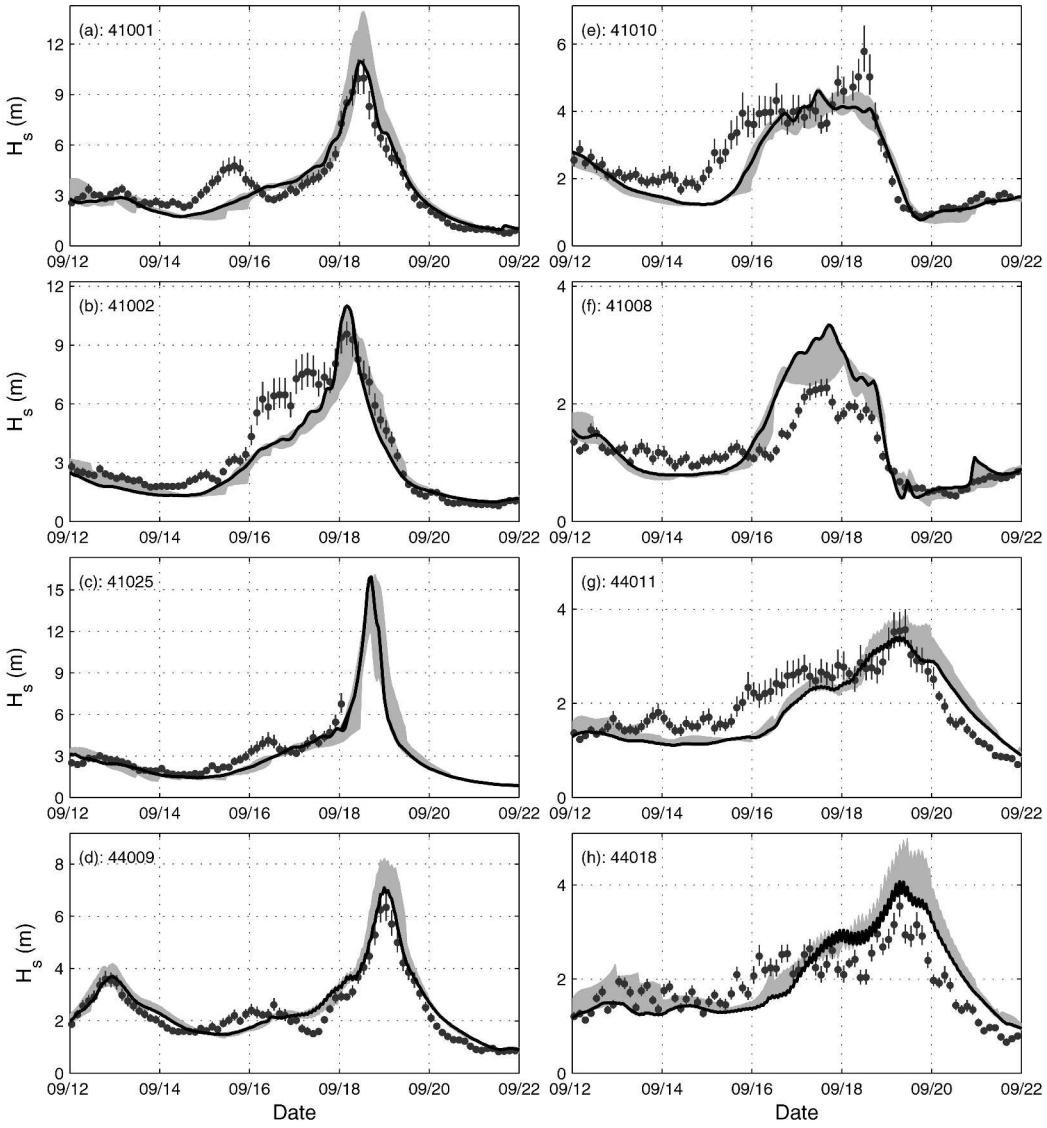

FIG. 7. As in Fig. 6 but for the WNA model.

7) are generally narrow, and in many cases are narrower than the 95% confidence intervals of the buoys. This indicates a generally excellent quality of the forecasts. This is furthermore confirmed by the bulk wave height statistics for the 48-h forecasts as presented in Table 3. For the most extreme wave conditions near the track of Isabel, the NAH forecasts (shaded area) systematically overestimate the hindcast wave heights (solid lines) and predict the most extreme conditions to occur too early (Figs. 6a–d). The magnitude of the errors, however, is generally less than 20% in height and less than 6 h in time for the entire 72-h forecasts. The corresponding errors in the WNA model (Figs. 7a–d) are similar in magnitude, but less systematic. For example, at buoy 41002 (Fig. 7b) the WNA forecasts systematically underestimates the hindcast. The timing of the most extreme conditions in the WNA model is excellent, with the forecasts being slightly late at buoys 41002 and 41025. The top three rows in Tables 2 and 3 show only a modest increase in model errors from the hindcasts to the 48-h forecast. Because the errors at these locations are dominated by the actual passages of Isabel, this is another indication of the good quality of the 48-h (wind and) wave forecasts.

In the swell dominated periods, the model forecasts are generally lower than the model hindcasts. This is consistent with the underestimation of wind speeds in the forecasts (Fig. 3). Anomalous behavior is found for

TABLE 2. Bulk statistics of hindcast model wave heights for all buoy locations.

		NAH model			WNA model		
Buoy	Depth (m)	Bias (m)	Rms (m)	SI (%)	Bias (m)	Rms (m)	SI (%)
41025	18.9	−0.01	0.68	23	−0.35	0.80	27
41001	4389	0.02	0.62	18	−0.05	0.79	23
41002	3786	−0.40	1.04	30	−0.57	1.02	29
41008	18.0	0.42	0.64	55	0.19	0.48	42
41012	38.4	0.30	0.47	26	0.06	0.34	19
41010	841.2	−0.03	0.48	18	−0.34	0.68	26
41009	42.0	0.07	0.44	20	−0.21	0.52	24
44009	28.0	0.26	0.38	16	0.18	0.41	17
44004	3164	0.30	0.69	26	0.21	0.78	29
44025	40.0	0.38	0.50	23	0.30	0.54	25
44017	52.4	0.24	0.43	20	0.14	0.44	20
44008	62.5	0.05	0.48	21	−0.04	0.64	28
44011	88.4	−0.04	0.37	18	−0.15	0.46	23
44018	56.7	0.21	0.42	23	0.10	0.55	29
44005	21.9	0.23	0.31	22	0.03	0.34	24

the northern buoys (Figs. 6g,h and 7g,h, and the bottom 8 rows in Tables 2 and 3), where the forecast wave heights are higher than the hindcast wave height. This is unexpected considering the systematic underestimation of forecast wind speeds. It appears to indicate that the forecast wind fields favor the highest wind speeds in more southerly directions compared to the wind analyses.

In the forecasts, systematically increasing wind errors are expected to result in systematically increasing wave model errors. This behavior can be observed when comparing the errors statistics for the hindcast (Table 2) with the error statistics for the 48-h forecast (Table 3). The modest increase of, particularly, the rms and SI confirms the generally good quality of the forecast. Note that the error growth with forecast time is larger in the WNA model for all buoys except for buoy 41008. This indicates that the superiority of the NAH model for forecasting Isabel's wave conditions increased with forecast time.

TABLE 3. As in Table 2 but for 48-h forecasts.

		NAH model			WNA model		
Buoy	Depth (m)	Bias (m)	Rms (m)	SI (%)	Bias (m)	Rms (m)	SI (%)
41025	18.9	0.10	0.55	19	−0.34	0.82	28
41001	4389	0.14	0.82	24	0.08	1.05	31
41002	3786	−0.17	1.12	32	−0.54	1.11	32
41008	18.0	0.36	0.61	52	0.10	0.40	34
41012	38.4	0.22	0.40	22	−0.04	0.34	19
41010	841.2	−0.12	0.56	22	−0.43	0.67	26
41009	42.0	−0.03	0.43	20	−0.32	0.56	26
44009	28.0	0.37	0.56	23	0.33	0.61	25
44004	3164	0.45	0.73	27	0.44	0.98	37
44025	40.0	0.51	0.61	28	0.52	0.76	35
44017	52.4	0.37	0.51	23	0.36	0.63	29
44008	62.5	0.18	0.50	22	0.16	0.77	34
44011	88.4	0.05	0.36	18	−0.04	0.50	25
44018	56.7	0.35	0.53	28	0.31	0.72	38
44005	21.9	0.33	0.43	30	0.18	0.51	36

Another way of assessing the quality of the forecasts is to compare wave height fields for a given valid time from several model cycles. Due to the potential of damage to life and property, a time period close to landfall is most interesting. Figure 8 shows wave height fields near landfall at 1200 UTC 18 September from the NAH model for the hindcast, and the corresponding 24-, 48-, and 72-h forecasts. In the hindcast (Fig. 8a), the maximum wave height is just over 16 m, and severe conditions with wave heights $H_s > 12$ m are concentrated in a well-defined area just offshore of Cape Hatteras. The $H_s = 4$ m contour, which is near the 12-ft threshold level used in the advisories of TPC, covers a large area. The extent of this contour from the center of Isabel varies enormously per quadrant, as noted in the advisories of TPC. The three forecasts valid for this time show similar height distributions and maximum wave heights, with the latter reaching the coastline around Cape Hatteras. The major difference is that the (GFDL) forecasts brings Isabel onshore somewhat too quickly. Figure 8, nevertheless, clearly shows the ability of the NAH model to provide accurate wave forecasts up to its forecast horizon of 72 h.

Figure 9 shows similar results from the WNA model. Qualitatively these are similar to the results of the NAH model, with the (GFS) forecasts taking Isabel to the shore at a slower pace. The WNA model forecast horizon is 7 days, and 4- and 5-day forecasts from the WNA model are also presented in Figs. 9e and 9f. For these forecasts, track and timing errors grow larger, as would be expected, but the structure, intensity, and general direction of Isabel's wave fields are captured well. Note that the maximum wave heights in both figures range from 15 to 18 m, consistent with the narrow envelopes of forecast wave heights at buoy locations in Figs. 6 and 7.

5. Discussion

We have discussed the wind–wave forecast guidance for Hurricane Isabel provided by NCEP's NAH and WNA model. The former model is a specialized hurricane wave model, using blended wind fields from the GFDL and GFS models. The latter model exclusively uses GFS wind fields. The NAH model provided excellent guidance for Isabel throughout her life cycle. For

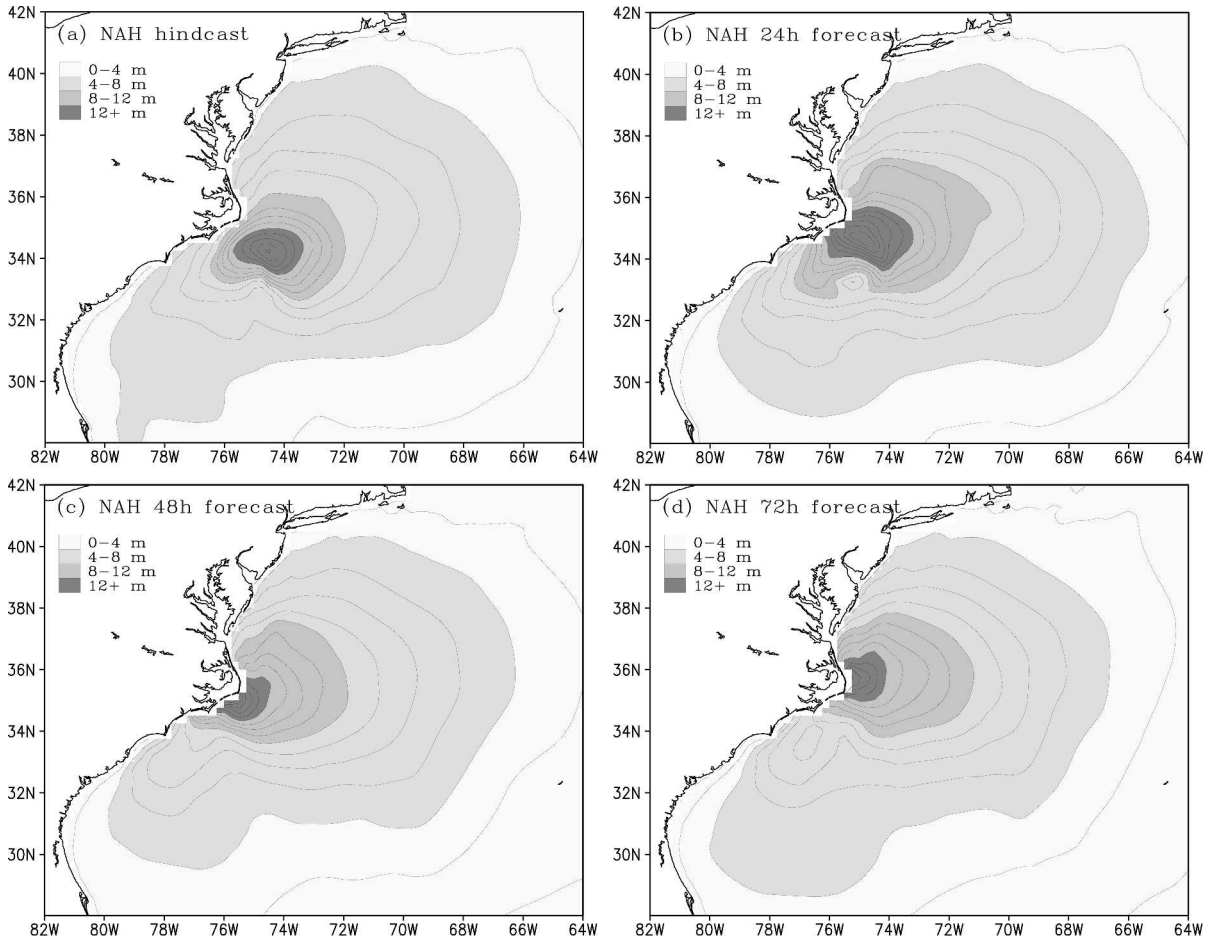

FIG. 8. Wave height fields from NAH model valid at 1200 UTC 18 Sep from (a) hindcast, (b) 24-h forecast, (c) 48-h forecast, and (d) 72-h forecast. Contours at 1-m intervals; shading as in legend.

buoys near the coast, the guidance was excellent up to the 72-h forecast horizon. The WNA model does not properly represent Isabel in its early stages, and does not accurately predict early swell arrivals at the buoys and at the coast. However, near landfall, the WNA model provides excellent guidance, well beyond the 72-h forecast horizon of the NAH model.

It should be noted that the good performance of the wave models is foremost due to the excellent quality of the wind fields. In many case studies, wind field errors dominate wave model errors up to an extent that it is impossible to isolate wave model errors. Whereas some major wave forecast deficiencies can still be attributed to errors in the wind fields, the latter are generally sufficiently accurate to allow for identification of shortcomings of the underlying wave model. Below we will discuss the following wave model issues in more detail: (i) wave model behavior in shallow water, (ii) prediction of extreme wave conditions, (iii) wave–current interactions, (iv) predictability of wave conditions, and (v) numerical issues. These issues all have a direct impact on the quality of the numerical wave guidance and represent possible avenues of further research.

The most obvious shortcoming of both wave models is the overestimation of the wave heights H_s in shallow water at buoy 41008 (Figs. 6f and 7f). Tentatively, this can be attributed to inadequate modeling of shallow water processes such as refraction and bottom friction. Because no small-scale spatial variability is found in altimeter data (see TAC), local focusing and shadow zones due to refraction are also not likely to be responsible for this behavior. However, the bottom friction coefficient as used in the wave models ($\Gamma = -0.019$ m^2 s^{-3}, Table 1) is smaller by a factor of 2–4 than traditionally recommended values (e.g., Hasselmann et al. 1973; Bouws and Komen 1983). This value was adopted to properly describe the extremely smooth shallow water areas in the Gulf of Mexico (information available online at http://polar.ncep.noaa.gov/waves/mod/bot1/). The bottom at the Atlantic shelf is, due to its exposure

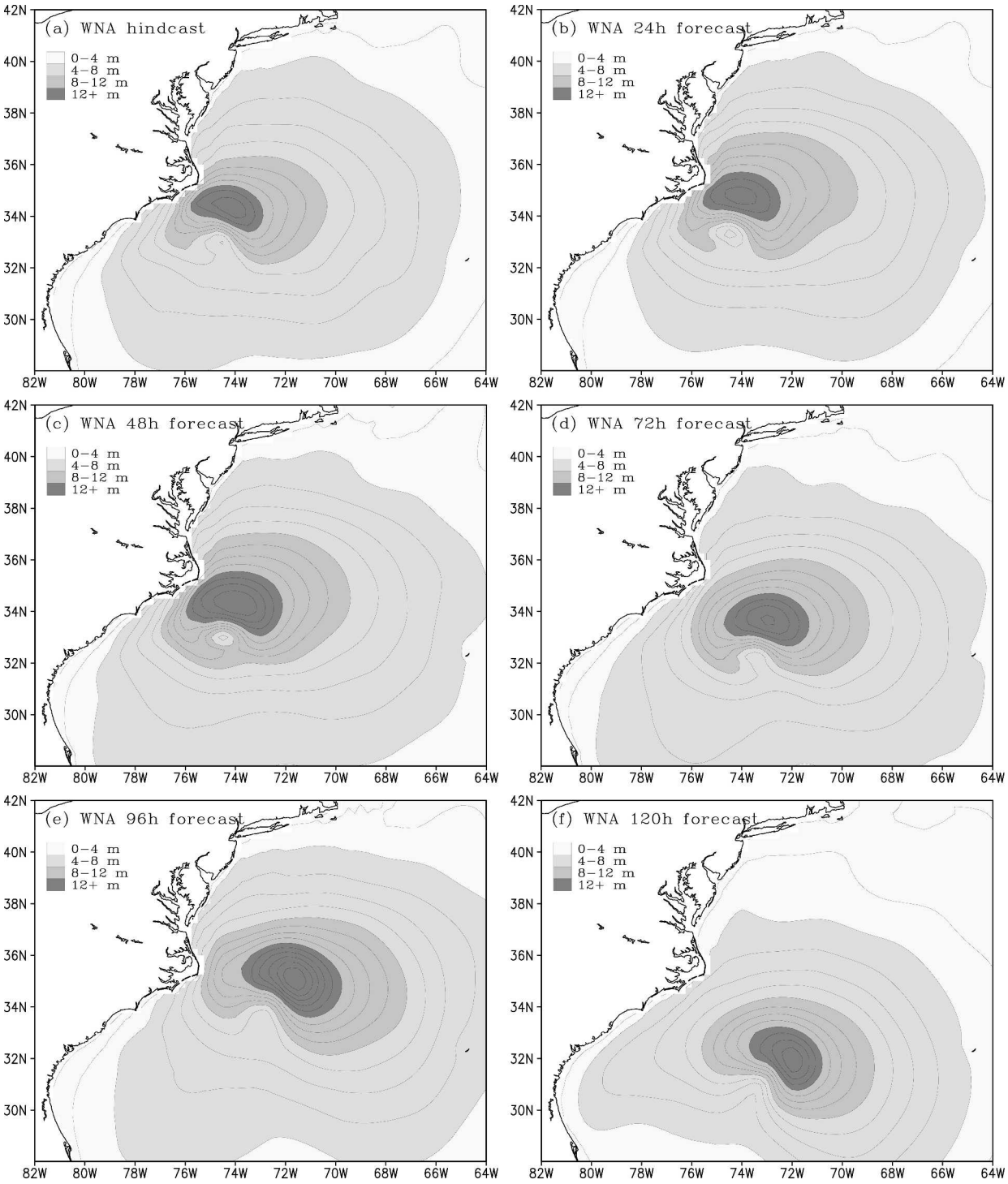

FIG. 9. As in Fig. 8 but for the WNA model, adding (e) 96- and (f) 120-h forecasts.

to longer period swells, rougher than the bottom in the Gulf of Mexico. The bottom friction setting in the model therefore is expected to result in an underestimation of the energy loss due to bottom friction at the Atlantic shelf. This appears to be the most likely explanation for the overestimation of the wave heights at buoy 41008.

The second issue that requires additional discussion is the prediction of waves in extreme wind conditions. Buoys rarely observe (and survive) such conditions. Al-

timeter data also prove sensitive to dropouts in hurricane wave conditions (e.g., Fig. 5). This makes the assessment of wave model performance in the most extreme conditions difficult. Nevertheless, some interesting observations can be made from the present data.

The altimeter track through the eye of Isabel on 13 September (Fig. 5a) occurs in a period in which the winds in the NAH model appear to be underestimated (Fig. 3), yet the corresponding wave heights are not underestimated. It can also be observed that near landfall the NAH winds appear to be of proper intensity, but cover an area that is too small, whereas the WNA winds appear to have the proper spatial scales, yet are too weak (Figs. 4 and 3). However, the corresponding wave heights near Isabel (Figs. 6a–d and 7a–d) do not appear to be underestimated as would be expected.

Both observations suggest that wave growth in hurricane conditions is too rapid in the wave model. This can tentatively be explained by recent observations of surface stresses in hurricane conditions. Wave growth rates scale with the corresponding friction velocity or drag coefficient (Tolman and Chalikov 1996). Common relations for the drag coefficient are based on observations in a narrow range of moderate wind speeds. Recent observations and theories (e.g., Powell et al. 2003; Moon et al. 2004*)* suggest that extrapolation of these relations to extreme conditions overestimate drag coefficients and stresses, and would hence overestimate wave growth rates. This represents a potential deficiency in the wave model physics.

The third issue that deserves further attention is the effect of wave–current interactions, which appears to be present in the observations from buoy 44018 (Figs. 6h and 7h). Note that these interactions are even more obvious in the buoy data at native resolution (see TAC, their Fig. 4.7c), and are also obvious in the spectral data (see TAC, their Fig. 5.2). In principle, such interactions can be included in the WAVEMATCH III model (e.g., Tolman 1991; Holthuijsen and Tolman 1991). This will, however, require an accurate model to describe near-surface mean currents that are due to tides, storm surges, and deep ocean circulation such as the Gulf Stream for the entire wave model domain. Such models are presently under development at NCEP.

The fourth issue deals with the predictability of hurricane waves. Conventionally, wave models are forced with relatively smooth and slowly varying wind fields. Combined with the fact that hyperbolic equations of a wave model represent a forced and damped physical system, chaotic behavior is generally not expected. Predictability is therefore generally not considered relevant and is generally not evident in wave modeling.

However, altimeter data away from the center of Isabel as presented in Fig. 5c show a distinct variability on small to moderate spatial scales, suggesting chaotic behavior. Moreover, the hourly GFDL wind fields show a distinct variability from hour to hour. Near the eye of Isabel, this also results in variability in the maximum wave height on an hourly time scale. These observations and model data therefore appear to indicate that predictability and chaotic behavior might be relevant for wind waves in hurricane conditions. The present operational wave modeling set up at NCEP does not allow us to investigate this subject further. We can therefore only identify this is an interesting new subject for wave research.

Finally, two numerical issues deserve additional attention. First, several buoys, particularly buoy 41018 in the NAH model (Fig. 6h), display noise in the model wave heights H_s with a period of two times the overall time step of the model (1 h). Normally, such noise is associated with numerical instabilities in the model. For WAVEWATCH III, it is suspected that this is due to the fact that the order of the spatial propagation and refraction computations is alternated per time step for numerical accuracy. For relatively well resolved fields, this indeed increases numerical accuracy. For poorly resolved fields, however, this introduces noise with a period of $2\Delta t$. Note that this is strictly noise and does not affect the numerical stability of the model. Second, several panels in Fig. 5 appear to display the so-called garden sprinkler effect (GSE), which points to a moderate disintegration of swell fields in discrete swell fields corresponding to the discretization $F(f, \theta)$ (Booij and Holthuijsen 1987; Tolman 2002b). The GSE is manifested by preferred wave propagation in the discrete spectral direction (15° intervals) from the major areas of wave generation. The GSE is much more apparent in plots of the peak period T_p (figures not presented here). Both issues can be addressed by minor tuning of existing numerical methods in the WAVEWATCH III model. We have investigated this in more detail using Isabel as a test case, and we have implemented some adjustments before the start of the 2004 Atlantic hurricane season (information available online at http://polar.ncep.noaa.gov/waves/changes.html).

6. Conclusions

The present manuscript addresses the accuracy of two operational wave models of NCEP for Hurricane Isabel. With many independent wind analyses, and wave observations from the *Jason-1* altimeter and 15 NDBC buoys, a rich validation dataset is available.

It is shown that the model specifically developed for

hurricane wave prediction (NAH) generally outperforms the "generic" WNA model, particularly when Isabel was a relatively small but intense category 5 hurricane. Both models show excellent forecasts for Isabel near landfall for the 72-h forecast horizon of the NAH model, and for several more days for the WNA model.

Major wave model deficiencies are shown to be related to deficiencies in the wind fields used to force the two models. However, it also appears that there is still room for improvement in the underlying generic wave model as discussed in section 5.

The present results also indicate that there may be limits to the predictability of hurricane swells. Such limits have not been encountered in wave modeling before, to the best knowledge of the present authors.

Acknowledgments. The authors would like to thank NDBC, in particular Dave Gilhousen and Richard Bouchard, and AOML, in particular Mark Powell, for their help with obtaining validation data and background information relevant to these data. We also would like to thank D. B. Rao, and the anonymous reviewers, for their comments on early drafts of this manuscript.

REFERENCES

Beven, J., and H. Cobb, 2003: Tropical cyclone report: Hurricane Isabel, 6–19 September 2003. National Weather Service. [Available online at http://www.nhc.noaa.gov/2003isabel.shtml.]

Booij, N., and L. H. Holthuijsen, 1987: Propagation of ocean waves in discrete spectral wave models. *J. Comput. Phys.,* **68,** 307–326.

Bouws, E., and G. J. Komen, 1983: On the balance between growth and dissipation in an extreme depth-limited wind-sea in the southern North Sea. *J. Phys. Oceanogr.,* **13,** 1653–1658.

Caplan, P., J. Derber, W. Gemmill, S.-Y. Hong, H.-L. Pan, and D. Parish, 1997: Changes to the 1995 NCEP operational medium-range forecast model analysis–forecast system. *Wea. Forecasting,* **12,** 581–594.

Chao, Y. Y., L. D. Burroughs, and H. L. Tolman, 2003a: The North Atlantic Hurricane wind wave forecasting system (NAH). Technical Procedures Bulletin 478, National Weather Service. [Available online at http://polar.ncep.noaa.gov/mmab/tpbs/tpb478/tpb478.htm.]

——, ——, and ——, 2003b: Wave forecasting for the western North Atlantic and adjacent waters. Technical Procedures Bulletin 495, National Weather Service. [Available online at http://polar.ncep.noaa.gov/mmab/tpbs/tpb495/tpb495.htm.]

——, J. H. G. M. Alves, and H. L. Tolman, 2005: An operational system for predicting hurricane-generated wind waves in the North Atlantic Ocean. *Wea. Forecasting,* **20,** 652–671.

Donelan, M., and W. J. Pierson, 1983: The sampling variability of estimates of spectra of wind-generated gravity waves. *J. Geophys. Res.,* **88,** 4381–4392.

Grumbine, R. W., 1996: Automated passive microwave sea ice concentration analysis at NCEP. OMB Tech. Note 120, National Weather Service, 13 pp.

Hasselmann, K., and Coauthors, 1973: Measurements of wind-wave growth and swell decay during the Joint North Sea Wave Project (JONSWAP). *Eng. Dtsch. Hydrogr. Z.,* **12A** (8), 95 pp.

Holthuijsen, L. H., and H. L. Tolman, 1991: Effects of the Gulf Stream on ocean waves. *J. Geophys. Res.,* **96,** 12 755–12 771.

Moon, I. J., T. Hara, I. G. S. E. Belcher, and H. L. Tolman, 2004: Effect of surface waves on air–sea momentum exchange. Part I: Effect of mature and growing seas. *J. Atmos. Sci.,* **61,** 2321–2333.

Moorthi, S., H. Pan, and P. Caplan, 2001: Changes to the 2001 NCEP operational MRF/AVN global analysis/forecast system. Technical Procedures Bulletin 484, National Weather Service. [Available online at http://www.nws.noaa.gov/om/tpb/.]

Powell, M. D., S. H. Houston, and T. A. Reinhold, 1996: Hurricane Andrew's landfall in south Florida. Part I: Standardizing measurements for documentation of surface wind fields. *Wea. Forecasting,* **11,** 304–328.

——, ——, L. R. Amat, and N. Morisseau-Leroy, 1998: The HRD real-time hurricane wind analysis system. *J. Wind Eng. Indust. Aerodyn.,* **77/78,** 53–64.

——, P. J. Vickery, and T. A. Reinhold, 2003: Reduced drag coefficient for high wind speeds in tropical cyclones. *Nature,* **442,** 279–283.

Ray, R. D., and B. D. Beckley, 2003: Simultaneous ocean wave measurements by the Jason and Topex satellites, with buoy and model comparisons. *Mar. Geod.,* **26,** 367–382.

Tolman, H. L., 1991: A third-generation model for wind waves on slowly varying, unsteady, and inhomogeneous depths and currents. *J. Phys. Oceanogr.,* **21,** 782–797.

——, 2002a: The 2002 release of WAVEWATCH III. Preprints, *Seventh Int. Workshop on Wave Hindcasting and Forecasting,* Banff, AB, Canada, Environment Canada, 188–197.

——, 2002b: Alleviating the garden sprinkler effect in wind wave models. *Ocean Modell.,* **4,** 269–289.

——, 2002c: User manual and system documentation of WAVEWATCH III version 2.22. Tech. Note 222, Ocean Modeling Branch, National Weather Service, 133 pp.

——, and D. V. Chalikov, 1996: Source terms in a third-generation wind–wave model. *J. Phys. Oceanogr.,* **26,** 2497–2518.

——, B. Balasubramaniyan, L. D. Burroughs, D. V. Chalikov, Y. Y. Chao, H. S. Chen, and V. M. Gerald, 2002: Development and implementation of wind-generated ocean surface wave models at NCEP. *Wea. Forecasting,* **17,** 311–333.

——, J. H. G. M. Alves, and Y. Y. Chao, 2004: A review of operational forecasting of wind generated waves by hurricane Isabel at NCEP. Tech. Note 235, Marine Modeling and Analysis Branch, National Weather Service, 45 pp.

Young, I. R., 1986: Probability distribution of spectral integrals. *J. Waterway Port Coastal Ocean Eng.,* **112,** 338–341.

——, 2003: A review of the sea state generated by hurricanes. *Mar. Structures,* **16,** 210–218.